



HHS Public Access

Author manuscript

Lab Chip. Author manuscript; available in PMC 2024 February 14.

Published in final edited form as:

Lab Chip. ; 23(4): 793–802. doi:10.1039/d2lc00970f.

Emulating clinical pressure waveforms in cell culture using an Arduino-controlled millifluidic 3D-printed platform for 96-well plates

Adam H. Szmelter,

Giulia Venturini,

Rana J. Abbed,

Manny O. Acheampong,

David T. Eddington

Department of Biomedical Engineering, University of Illinois at Chicago, 835 S. Wolcott Ave. Chicago, IL, USA.

Abstract

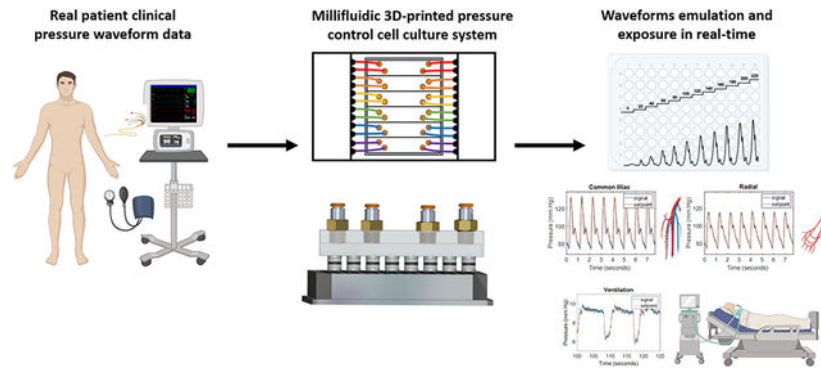
High blood pressure is the primary risk factor for heart disease, the leading cause of death globally. Despite this, current methods to replicate physiological pressures in-vitro remain limited in sophistication and throughput. Single-chamber exposure systems allow for only one pressure condition to be studied at a time and the application of dynamic pressure waveforms is currently limited to simple sine, triangular, or square waves. Here, we introduce a high-throughput hydrostatic pressure exposure system for 96-well plates. The platform can deliver a fully-customizable pressure waveform to each column of the plate, for a total of 12 simultaneous conditions. Using clinical waveform data, we are able to replicate real patients' blood pressures as well as other medically-relevant pressures within the body and have assembled a small patient-derived waveform library of some key physiological locations. As a proof of concept, human umbilical vein endothelial cells (HUVECs) survived and proliferated for 3 days under a wide range of static and dynamic physiologic pressures ranging from 10 mm Hg to 400 mm Hg. Interestingly, pathologic and supraphysiologic pressure exposures did not inhibit cell proliferation. By integrating with, rather than replacing, ubiquitous lab cultureware it is our hope that this device will facilitate the incorporation of hydrostatic pressure into standard cell culture practice.

Graphical Abstract

dte@uic.edu .

Conflicts of interest

There are no conflicts to declare.



Clinical pressure waveforms are introduced into cell culture using a millifluidic 3D-printed platform.

1 Introduction

Cells within the body are subject to a wide range of mechanical stimuli such as compression, stretch, shear stress, and hydrostatic pressure (HP). These microenvironmental cues are crucial for regulating cellular functions such as migration¹, apoptosis², proliferation³, and differentiation⁴. Among these mechanical cues, HP is perhaps the least investigated due to challenges in implementing pressure into cell culture. Hydrostatic pressure has been found to be crucial for homeostasis and development in the cardiovascular system, central nervous system, immune system, eye, bladder, and cartilage⁵. Each organ, tissue, and cell type experiences a distinct hydrostatic pressure waveform; each with a unique amplitude, frequency, and shape. The uniqueness of each waveform is a function of several parameters; these include the organ or tissue's biomechanical environment and compliance, the source of the pressure (for most tissues, this is the heart), the distance from the source pressure, fluid status, and local pressure regulatory mechanisms. Paradoxically, despite the wide variety in hydrostatic pressure seen throughout the body, local disturbances or alterations in hydrostatic pressure are known to cause tissue damage and disease. Most notably, high blood pressure, or hypertension, is the primary risk factor for heart disease, the leading cause of death globally.

Three techniques have been previously used to modulate HP *in vitro*; the syringe method, the media height method, and the gas pressure method. These techniques all suffer from a critical drawback—only one pressure condition may be delivered at a time. The syringe method applies pressure through a fluidic path pressurized by a syringe pump. This is advantageous because of the ability to deliver negative pressure and positive pressures, however, due to its closed nature, there is not a way to maintain 5% CO₂ and 21% O₂ thus limiting the length of experiments and requiring special media. The cell media height method applies pressure through a water column and is simple and easy to implement; however, a major drawback is that pO₂, pH, and pCO₂ all change significantly with media height due to Henry's law⁶. To correct for this, systems have been designed that flow a gas-equilibrated solution over the cells⁷; however, the flow introduces shear stress whose effects cannot be decoupled from HP. The gas pressurization method pressurizes the headspace

above the cell culture media thus maintaining stable gas concentrations without requiring flowing media. Also, HP may be cyclically controlled using electronic pressure regulators and valves⁸. This method most resembles our method with several key differences: 1) the pressure chambers are bulky, custom-built devices that supply a single pressure condition at a time 2) they are not compatible with standard high-throughput biomedical research tools such as plate readers⁹⁻¹¹, and 3) pressure control waveforms, when implemented, are limited to sinusoidal, triangular, and square waves^{8,10}, which do not resemble those experienced by cells in-vivo. However, recent advances in open-source microfluidic pressure control¹² and methods developed by our laboratory to control gaseous environments within the headspace of 96-well plates¹³ have set the stage for precise control of complex waveforms within cell culture. Building on the strengths of the gas pressure method and overcoming its weakness, we introduce a high-throughput, workflow-compatible, precise-waveform device for in-vitro hydrostatic pressure control in 96-well plates.

2 Methods

2.1 Device construction and assembly

As shown in Figure 1, the device consists of 12 distinct pressure lines, each controlled by a proportional solenoid valve and a pressure sensor. A pressure source (gas cylinder, pump, or compressor) is connected to two 8-station gas manifolds (Parker Legris) via $\frac{1}{4}$ " push-to-connect fittings. Unused manifold outputs are blocked using cap plugs, and 12 outputs are connected to the inlets of the proportional solenoid valves using $\frac{1}{8}$ " pneumatic tubing. Each valve (Parker VSO LowPro) is mounted on a single-station manifold with $\frac{1}{16}$ " National Pipe Thread (NPT) to $\frac{1}{8}$ " push-to-connect adaptors. The inlet is fitted with a single connection while the outlet utilizes a wye adaptor to split flow between the inlet of the 3D-printed insert and a pressure vent. The vent rate is controlled by an IV flow regulator that can be adjusted manually depending on the waveform. Static pressure conditions may be set to near closed while dynamic pressure conditions will require more venting to allow pressure to escape. The pressure within the system is read by a piezoresistive pressure sensor (Honeywell 40PC series) every 1 ms and relayed to an Arduino Mega 2560 microcontroller that uses a PID feedback control algorithm to open and close the valve accordingly to achieve the desired setpoint pressure. Proportional solenoid valves open proportionally to the applied voltage set by the microcontroller. Using Pulse Width Modulation (PWM) at 480 Hz, analog voltage waveforms may be approximated using digital signals. Here, an individual PWM signal controls each valve through an IRF 520 MOSFET driver module connected to 12V DC power. The microcontroller is programmed using MATLAB Simulink and the Simulink Support Package for Arduino Hardware. The Arduino Mega 2560, due to memory limitations, can only control 6 simultaneous pressure conditions. For this reason, two microcontrollers were used for waveform PID control and a third was used to visualize all 12 waveforms. Device components and wiring are shown in Figure 2.

2.2 Millifluidic 3D-printed inserts and O-rings

Each millifluidic 3D-printed insert fits into the wells of a single column of a 96-well plate. Pressurized gas enters the device through $\frac{1}{8}$ " pneumatic tubing inserted into a push-to-connect fitting. This fitting allows for easy insertion and removal of tubing and is screwed onto the device using 3D-printed $\frac{1}{16}$ " NPT threads. From here, gas flows into a central 7x5x75 mm 8-channel rectangular millifluidic manifold. Gas is then distributed amongst 8 rectangular millifluidic 2x2x7 mm channels that flow into the individual wells of a column of the 96-well plate. The device outlet is connected to a pressure sensor (Figure 2C) also through a $\frac{1}{16}$ " NPT to $\frac{1}{8}$ " push-to-connect adaptor. A gas-tight seal is created using a radial O-ring design. A single Buna-N O-ring fits into a groove 3D-printed on each column of the device. O-rings are X-profile for greater sealing surface area and PTFE backup rings are positioned above and below the O-rings to prevent extrusion during insertion (Figure 3C-F).

2.3 Millifluidic well plate insert fabrication

Millifluidic 3D-printed pressure control inserts were designed in Solidworks and printed using a stereolithographic 3D printer (Form 3, Formlabs) at a 25 μm layer height. Prints were then washed in 100% isopropanol in the Formlabs Formwash resin removal device. Internal channels were washed with a syringe fitted with a $\frac{1}{16}$ " NPT-to-leur adaptor. Next, the device was dried with compressed air and cured for 1 hour at 60° C in the Formlabs Formcure curing device. $\frac{1}{16}$ " NPT to $\frac{1}{8}$ " push-to-connect pneumatic adaptors were screwed into the device and sealed with resin and cured for 1 hour to ensure no leakage along the thread's spiral leak path. The 3D-printed insert sits above the media in the well and pressurizes the headspace of each well.

2.4 Device validation: pressure measurement within each well

To validate that the pressure applied to each column of the plate is the same as the pressure within in each well, holes were drilled so that a pressure sensor could be directly inserted into each cavity. This way, pressure could be compared to the pressure applied to that column as a whole. Holes were drilled with a Dremel tool and sensors were inserted through a 10 mm long section of $\frac{1}{8}$ " polyurethane tubing into the well. The tubing was sealed to the well plate using a cyanoacrylate adhesive. Pressure was then measured within each well at a range from 0-50 psi and compared to the input pressure that is measured downstream of the 3D-printed insert as shown in Figure 3.

2.5 Simultaneous pressure waveforms

To demonstrate the generation of a spectrum of waveforms, 12 simultaneous pressure waveforms found in the circulation were generated within a single 96-well plate (Figure 4). Each column of the plate was supplied by a different dynamic pressure waveform. Waveforms generated ranged from 12/8 mm Hg to 270/180 mm Hg. Pressure waveforms produced were 12/8, 24/16, 30/20, 40/26, 60/40, 90/60, 120/80, 150/100, 180/120, 210/140, 240/160, and 270/180 mm Hg as shown in Figure 4.

2.6 Clinical waveform selection

Patient waveforms were obtained from clinical online databases, medical journals, or academic papers in which waveforms were simulated based on physiological data. The source of each waveform can be found in Table 1. Eleven anatomically specific arterial pressure waveforms (Figure 5) were downloaded from a database of virtual healthy subjects¹⁴. Iliac, femoral, anterior tibial, ascending aorta, aortic bifurcation, radial, aortic root, descending aorta, thoracic aorta, carotid, and brachial arteries were selected. Intracranial pressure waveforms (Figure 6) were downloaded from the Cerebral Haemodynamic Autoregulatory Information System Database (CHARIS DB), which contains data from surgical intensive care unit rooms at Robert Wood Johnson medical center. This data contains continuous ICP measurements from intra-parenchymal micro transducers with a resolution of .14 mm Hg and dynamic range of 500 mm Hg^{15,16}.

2.7 Clinical waveform emulation

Time and pressure data from waveforms were imported into MATLAB and clipped to single-period segments. These segments were set to repeat infinitely using the "repeating sequence" command and were used as dynamic setpoints for the PID control algorithm. Pressure signal, setpoint, and error data for each waveform were collected for 30 seconds for plotting and error analysis. Waveforms are shown in Figures 5 and 6 and average full-scale error is shown in 7. This is the percent error relative to the sensor's full measurement range.

2.8 Cell culture and viability measurement

Human umbilical vein endothelial cells (Lonza) were grown in EGM-2 media (Lonza) at 37C and 21% O₂ and 5% CO₂. They were split at 80% confluence at a ratio of 1:3 at passage numbers 1-5. Cells were seeded at 15,000 cells/well in a 96-well plate 24 hours before pressure exposure. Viability was measured every 8 hours using PrestoBlue High Sensitivity Cell Viability Reagent (ThermoFisher) according to manufacturer instructions using a plate reader (Varioskan, Thermo Scientific) at 560/590 nm excitation/emission (bottom read).

3 Results and discussion

3.1 Principle of device operation

HP at the cell surface is controlled by pressurizing the headspace of each well. According to Pascal's law, pressure applied from the atmosphere is equally transmitted in all directions throughout the fluid, as shown in Fig. 1D. Due to its incompressible nature, we expect that cell media will act as a suitable alternative for human blood as it has been found to have a similar compressibility to water, regardless of hematocrit²². The cell culture hydrostatic pressure control platform consists of two main components: 1) the control hardware consisting of valves, sensors, and microcontrollers (Figure 2A), and 2) the 3D insert devices, which seal the wells of each column of a 96-well plate (Figure 1). Each pressure line has a dedicated valve, sensor, and vent. A PID control algorithm running on an Arduino microcontroller reads the pressure from the sensor, and opens or closes the valve accordingly to minimize the error from the setpoint. If pressure is below the setpoint, the

valve will open to let pressure build within the wells, and if pressure exceeds the setpoint, the valve will close, allowing it to vent. A pressurized cylinder or pump may be used as source pressure as long as cell culture gas (21% O₂ and 5% CO₂) is provided. The 3D-printed device seals to the well using a pressure-resistant X-profile O-ring design (Figure 3C-F). Each column connects to the control hardware through an inlet, which receives pressure from the valve, and an outlet, which connects to the pressure sensor (Figure 2C).

3.2 Device validation and pressure limits

Each column of the 96-well plate was set to a static pressure ranging from 2.5 to 50 psi and pressure within each well was measured (Figure 3). Pressure set points in each column were 2.5, 5, 7.5, 10, 15, 20, 25, 30, 35, 40, 45, and 50 psi. Well-to-well pressure values were consistent with an average standard deviation of 0.2 psi and an average of 0.2% full-scale error. Burst pressure is the pressure needed to dislodge the 3D-printed insert from the plate. The average burst pressure was 86.3 psi with a standard deviation of 5.6 psi.

3.3 Patient-derived pressure waveform library

Clinical waveforms emulated by our platform closely match setpoint values and are within all 2% full-scale error (Figure 7). Figure 5 shows arterial pressure waveforms from arteries throughout the body. Time and pressure (x,y) data was downloaded from a database of virtual healthy subjects¹⁴ while Figure 6 shows waveforms downloaded individual clinical databases (patient monitors), medical journals, as well as simulated waveforms from academic articles. Details regarding waveform origin are found in Table 1. The system demonstrates the ability to replicate waveforms from across the body with a high degree of accuracy.

3.4 Cell viability testing

HUVECs were grown under 12 pressure conditions within a 96-well plate. Each column received a unique pressure, either static or dynamic. Dynamic waveforms followed the shape of the arterial blood pressure waveforms shown in Figure 4 and were cycled at a frequency of 1 Hz. The dynamic waveforms generated were 20/10-, 80/60-, 120/80-, 200/100-, and 300/200-mm Hg. These pressures represent those found in the venous system (20/10 mm Hg), arterial hypotension (80/60 mm Hg), normotension (120/80 mm Hg), hypertension (200/100 mm Hg), and supraphysiologic hypertension (300/200 mm Hg). Static pressures included 25-, 50-, 100-, 150-, 200-, 300-, and 400-mm Hg. Cells in all conditions appeared to show comparable or even slightly enhanced growth compared to a control column that was grown at atmospheric pressure (Figure 8).

3.5 Discussion

In recent years, methods for cell culture within multiwell plates have grown increasingly complex and more accurate at mimicking in-vivo conditions. By incorporating micro and millifluidic elements, insert devices and custom-made plates now can incorporate a growing number of physiological variables such as gas tension^{13,23-25}, perfusion²⁶, matrix-stiffness²⁷, mechanical confinement^{28,29}, and cell-cell interaction³⁰. Multiwell plates are a powerful tool to investigate many conditions simultaneously and are the workhorse for

high-throughput screening. Our device seeks to integrate with, rather than replace, these ubiquitous consumables and to add another functionality—hydrostatic pressure.

Hydrostatic pressure is a key physiological variable. In the clinical setting, it is used to monitor patient status; in-vitro, it has been shown to be a regulator of important cellular processes such as proliferation, migration, apoptosis, and differentiation⁵. On the human scale, elevated blood pressure is the number one risk factor for heart disease—the leading cause of death and disability worldwide³¹. In the vascular system, endothelial cells experience the effects of both shear stress and hydrostatic pressure, however, the effects of pressure are difficult to decouple in in-vivo studies. Hydrostatic pressure has been studied as a variable in cell culture for at least two decades, however, current methods allow only a single pressure condition to be studied at a time thus greatly reducing throughput. Furthermore, several studies have shown contrasting evidence regarding the proliferation and apoptosis of endothelial cells in cell culture depending on the pressure magnitude, frequency, and exposure time³²⁻³⁸. Our device may be used to help resolve these discrepancies by providing a platform for simultaneous studies of up to 12 independent pressure waveforms, each with fully customizable magnitude, frequency, and duration.

To validate our system, first, it was important to verify that the pressure within each well was the same as the pressure setpoint supplied to each column. One-by-one, each well was verified to be within the sensor's margin error of our setpoint value (Figure 3). Each column maintained a unique static pressure from 2.5-50 psi. A high burst pressure of 86.3 psi ensures that cells can be exposed to almost all physiological pressures experienced in the body with the exclusion of pressures experienced within the joints during movement or from external trauma. The x-profile O-ring design and PTFE backup rings used in this device allow for easier insertion and removal as well as a 30 psi improvement in burst pressure compared to our previous work¹³.

Next, to validate that our platform was compatible with cell growth, we grew HUVECs under a full physiologic spectrum of both static and dynamic pressure profiles. To our surprise, cells under all conditions grew at a comparable or even slightly faster rate than controls. There was no significant difference between pressure conditions or between static and cyclic exposures. Static exposures ranged from 25 mm Hg to 400 mm Hg and cyclic pressures from 20/10 to 300/200 mm Hg. Pressures at the upper end of this spectrum (300/200 mm Hg dynamic pressure and 400 mm Hg static) exceed physiological levels. The highest blood pressure ever recorded was 370/360 mm Hg³⁹ (during a heavy weight-lifting exercise) and pressures above 180/120 mm Hg are considered a life-threatening hypertensive emergency. Therefore, after 3 days of exposure, it is surprising that cells grown under these conditions do not show a significant decrease in proliferation. To our knowledge, this is the first-time endothelial cells have been exposed to such high pressures in-vitro. Others have observed magnitude-dependent increases in proliferation measured via synthetic nucleoside bromodeoxyuridine (BrdU) uptake at 50-, 100-, and 150-mm Hg for 24 hours³² but exposure above 200 mm Hg has yet to be reported for endothelial cells. Shin et al. also found increased BrdU uptake with cyclic exposure at 60/20 and 100/60 but this effect decreased once pressures reached 140/100 mm Hg for 24 hours³⁵. Others have reported profound apoptosis at 200/100 mm Hg³⁸. In this work, PrestoBlue™ Cell Viability Reagent was used.

It is a resazurin-based dye that is reduced by metabolically active live cells. While this method is not as direct a measure of proliferation as BrDu uptake, increases in fluorescence directly correlate with cell concentration⁴⁰. Furthermore, this assay is non-destructive and plate reader-friendly, permitting for simultaneous continuous monitoring of cell growth in all 12 conditions over 3 days. A possible reason for the pronounced growth seen in our cells could be due to the method of pressure exposure. Using the gas pressurization method, the headspace is filled with 21% O₂ and 5% CO₂ from a pressurized tank. The increased headspace pressure results in increased solubility of both gases in the media according to Henry's law. Thus, the increased metabolism of Prestoblue could be at least partially a result of increased O₂ dissolved in the media. Even so, cell death was not observed in our system.

To our knowledge, this is the first example of control over multiple hydrostatic pressure conditions within a single cell culture platform. To illustrate this, we applied a spectrum of physiologic pressure waveforms ranging from 12/8 mm Hg to 270/180 mm Hg within a single 96-well plate (Figure 4). The ability to investigate multiple conditions simultaneously is essential for researchers seeking to optimize or explore even a modest experimental parameter space, which can be extremely time-consuming and laborious using single-chamber exposure methods. In bone and cartilage tissue engineering, HP has been found to be crucial for stem cell differentiation. Stavenschi et al. sought to determine which hydrostatic pressure magnitudes, frequencies, and exposure times would result in the most robust lineage commitment for bone marrow stem cells (hBMSCs)⁴¹. The study exposed hBMSCs to 3 pressure magnitudes, cycle frequencies, and durations. A single-condition pressure chamber was used for all experiments. Fully exploring this parameter space would require 27 experiments, not including controls or technical and biological replicates. Including 3 technical and 3 biological replicates, this would be 243 experiments. Using our 96-well pressure adaptor, the entire parameter space, including technical replicates and controls, can be condensed into a single experiment—with biological replicates, this becomes 3 experiments. This represents almost two orders of magnitude (81x) savings in time and resources.

Unlike commercial industrial pressure controllers, our platform is completely customizable in that raw x,y (time, pressure) data can be directly imported from patient monitors or clinical databases. To our knowledge, this is the first demonstration of an in-vitro cell culture system capable of exposing cells to real clinical pressure waveforms. Figures 5 and 6 show a library of clinical waveforms reproduced by the system with very low (<2%) full-scale error. The waveforms were downloaded from publicly available clinical databases and academic journals and represent various arterial and venous pressures, intracranial pressure, intraocular pressure, and ventilator-produced positive end-expiratory pressure (PEEP). Virtually any measured patient waveform or pressure signal can be produced by the system. This has potential for precision medicine applications, in which patient tissue samples can be grown and tested for chemotherapeutic efficacy in a pressure environment taken directly from clinical measurements. This is especially relevant for treating multidrug-resistant tumors which have been shown to upregulate specific drug efflux transporters in response to increased interstitial hydrostatic pressure⁴². Interstitial fluid pressure (IFP) measurements taken directly from a patient's tumor microenvironment could be used to grow patient samples and more accurately test for drug susceptibility. We acknowledge

that our system applies pressure within rigid-bottom multiwell plates and that the human body is comprised of tissues with varying stiffness and distensibility. We are excited by the potential to mimic these properties by incorporating 3D matrices and/or flexible bottom 96-well plates. This opens the door to further mechanobiological investigation of stretch and strain. This may be of particular interest to the study of ventilator-induced lung injury in which positive pressure causes overdistension and damage to the lung parenchyma.

4 Conclusions

The results presented here demonstrate a method for high-throughput hydrostatic pressure stimulation within 96-well plates. Previously limited to a single pressure condition at a time, researchers may now expose cells to 12 unique pressure profiles simultaneously—thus allowing for optimization and dose-response studies on a single 96-well plate. Using 3D printing, we fabricated a millifluidic insert device that creates a pressure-resistant, gas-tight environment within each well of the plate. By pressurizing the headspace, we can apply HP from above thus limiting undesirable contact with cell media. Arduino microcontrollers allow for fully customizable control of pressure profiles within the plate. Using this, we applied real clinical patient pressure waveforms to cells growing in culture for the first time. This method may have applications in precision medicine in which cells taken from patients' tissues may undergo chemotherapeutic efficacy testing under native pressure conditions to overcome pressure-induced chemoresistance.

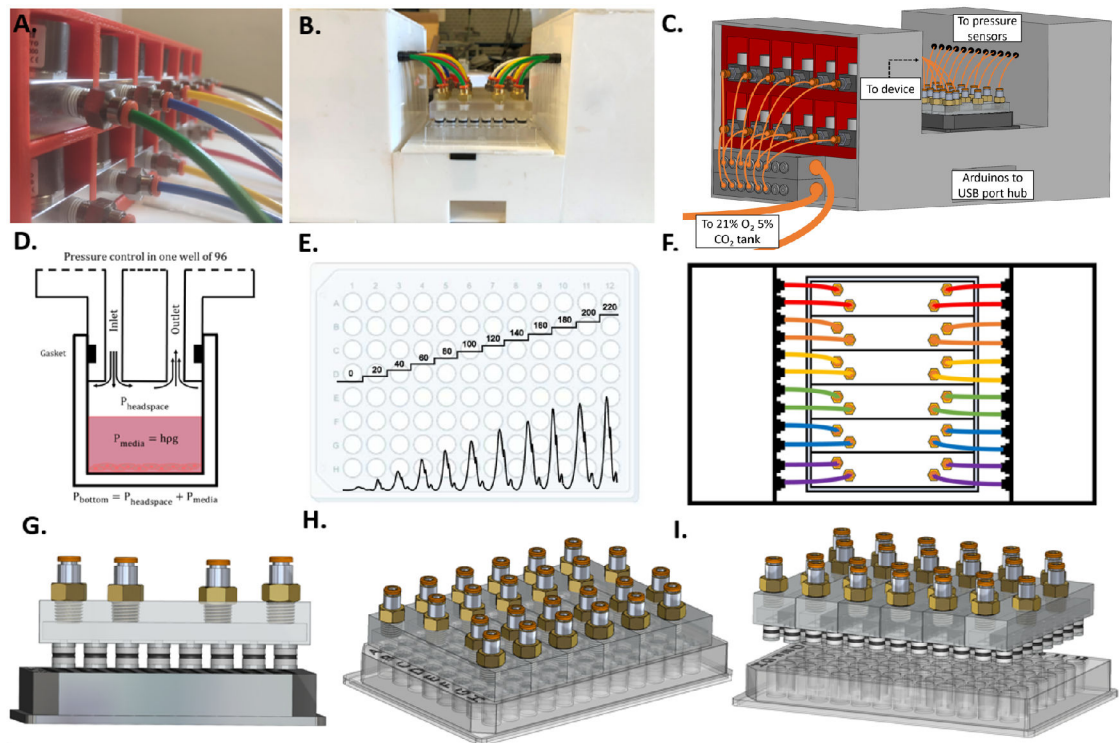
Acknowledgements

We gratefully acknowledge the financial support from the NIH under award number R21EB024003, and the American Heart Association Predoctoral Fellowship Award 20PRE3508008 for Adam Szmelter.

References

1. Xia Y, Pfeifer CR and Discher DE, *Acta Mechanica Sinica/Lixue Xuebao*, 2019, 35, 299–308.
2. Wu Y, van der Schaft DW, Baaijens FP and Oomens CW, *Journal of Biomechanics*, 2016, 49, 1071–1077. [PubMed: 26961799]
3. Vining KH and Mooney DJ, *Nature Reviews Molecular Cell Biology* 2017 18:12, 2017, 18, 728–742.
4. Wolfe RP and Ahsan T, *Biotechnology and Bioengineering*, 2013, 110, 1231–1242. [PubMed: 23138937]
5. Liu S, Tao R, Wang M, Tian J, Genin GM, Lu TJ and Xu F, *Applied Mechanics Reviews*, 2019, 71, year.
6. Haberstroh KM, Kaefer M, Retik AB, Freeman MR and Bizios R, *The Journal of urology*, 1999, 162, 2114–2118. [PubMed: 10569598]
7. Mandal A, Shahidullah M and Delamere NA, 2010, 51, 3129–3138.
8. Stover J and Nagatomi J.
9. Becquart P, Cruel M, Hoc T, Sudre L, Pernelle K, Bizios R, Logeart-Avramoglou D, Petite H and Bensedhoum M, *European Cells and Materials*, 2016, 31, 160–173. [PubMed: 26895242]
10. Rieder B, Weihs AM, Weidinger A, Szwarc D, Nürnberger S, Redl H, Rünzler D, Huber-Gries C and Teuschl AH, *Scientific Reports*, 2018, 8, 17010. [PubMed: 30451865]
11. Saha A, Rolfe R, Carroll S, Kelly DJ and Murphy P.
12. Watson C and Senyo S, *HardwareX*, 2019, 5, year.
13. Szmelter A, Jacob J and Eddington DT, *Analytical Chemistry*, 2021, *acs.analchem.0c04627*.

14. Willemet M, Chowienczyk P and Alastruey J, American Journal of Physiology - Heart and Circulatory Physiology, 2015, 309, H663. [PubMed: 26055792]
15. Kim N, Krasner A, Kosinski C, Winger M, Qadri M, Kappus Z, Danish S and Craelius W, Journal of clinical monitoring and computing, 2016, 30, 821–831. [PubMed: 26446002]
16. Goldberger AL, Amaral LA, Glass L, Hausdorff JM, Ivanov PC, Mark RG, Mietus JE, Moody GB, Peng CK and Stanley HE, Circulation, 2000, 101, year.
17. Johnson AE, Pollard TJ, Shen L, Lehman LWH, Feng M, Ghassemi M, Moody B, Szolovits P, Anthony Celi L and Mark RG, Scientific Data, 2016, 3, year.
18. Hill BL, Rakocz N, Rudas, Chiang JN, Wang S, Hofer I, Cannesson M and Halperin E, Scientific Reports, 2021, 11, year.
19. Moorhead LC, Gardner TW, Lambert HM, O'Malley RE, Willis AW, Meharg LS and Moorhead WD, Archives of Ophthalmology, 2005, 123, 1514–1523. [PubMed: 16286613]
20. Ma R, Hunter P, Cousins W, Ho H, Bartlett A, Safaei S and Renfei Ma C, 2019.
21. CPAP Pressure and Flow Data from a Local Trial of 30 Adults at the University of Canterbury v1.0.1, <https://physionet.org/content/cpap-data-canterbury/1.0.1/>.
22. Sacks AH and Tickner EG, Biorheology, 1968, 5, year.
23. Oppegard SC, Blake AJ, Williams JC and Eddington DT, Lab on a Chip, 2010, 10, 2366. [PubMed: 20689862]
24. Brennan MD, Rexius-Hall ML and Eddington DT, PLoS ONE, 2015, 10, year.
25. Gao X, Wei T, Chen J, Ai J, Jin T, Cheng L, Liu Y, Xiao K, Zeng X and Wang K, Biochemical and Biophysical Research Communications, 2018, 503, 2499–2503. [PubMed: 30208517]
26. Domansky K, Inman W, Serdy J, Dash A, Lim MH and Griffith LG, Lab on a Chip, 2010, 10, 51–58. [PubMed: 20024050]
27. Pushkarsky I, Tseng P, Black D, France B, Warfe L, Koziol-White CJ, Jester WF, Trinh RK, Lin J, Scumpia PO, Morrison SL, Panettieri RA, Damoiseaux R and Di Carlo D, Nature Biomedical Engineering, 2018, 2, 124–137.
28. Le Berre M, Zlotek-Zlotkiewicz E, Bonazzi D, Lautenschlaeger F and Piel M, Methods in Cell Biology, 2014, 121, 213–229. [PubMed: 24560512]
29. Kittur H, Weaver W and Di Carlo D.
30. Berry SB, Zhang T, Day JH, Su X, Wilson IZ, Berthier E and Theberge AB, Lab on a Chip, 2017, 17, 4253–4264. [PubMed: 29164190]
31. Oparil S, Czarina Acelajado M, Bakris GL, Berlowitz DR, Cífková R, Dominiczak AF, Grassi G, Jordan J, Poulter NR, Rodgers A and Whelton PK, Nature Publishing Group, 2018, 4, year.
32. Ohashi T, Sugaya Y, Sakamoto N and Sato M, Journal of Biomechanics, 2007, 40, year.
33. Hasel C, Dürr S, Brüderlein S, Melzner I and Möller P, Journal of Biomechanics, 2002, 35, 579–584. [PubMed: 11955497]
34. Schwartz EA, Bizios R, Medow MS and Gerritsen ME, Exposure of Human Vascular Endothelial Cells to Sustained Hydrostatic Pressure Stimulates Proliferation Involvement of the V Integrins, 1999.
35. Shin HY, Gerritsen ME and Bizios R, 2002.
36. Shin HY, Bizios R and Gerritsen ME, <http://dx.doi.org.proxy.cc.uic.edu/10.1080/10623320390237883>, 2009, 10, 179–187.
37. Yoshino D, Funamoto K, Sato K, Sato M and Teck Lim C.
38. Hasel C, Dürr S, Bauer A, Heydrich R, Brüderlein S, Tambi T, Bhanot U and Möller P, American Journal of Physiology - Cell Physiology, 2005, 289, year.
39. Narloch JA and Brandstater ME, Archives of physical medicine and rehabilitation, 1995, 76, 457–462. [PubMed: 7741618]
40. Reader V, assets.fishersci.com.
41. Stavenschi E, Corrigan MA, Johnson GP, Riffault M and Hoey DA, Stem Cell Research and Therapy, 2018, 9, 1–13. [PubMed: 29291747]
42. Shang M, Lim SB, Jiang K, Yap YS, Khoo BL, Han J and Lim CT, Lab on a Chip, 2021, 21, 746–754. [PubMed: 33502419]

**Fig. 1.**

Cell culture hydrostatic pressure platform A. Twelve proportional solenoid valves used to control the pressure within each column of the plate. B. Photograph of the platform connected to a 96-well plate. C. 3D CAD drawing of the platform with the left panel removed to show pneumatic connections to valves. D. Illustration of pressure control within a single well. E. Example of possible pressure profiles (dynamic or static) within a 96-well plate. F. Diagram of top-view of platform. G. 3D CAD drawing of front-view of insert device out of plate showing O-rings. H. 3D CAD drawing of device inserted into plate. I. 3D side-view CAD drawing of device out of plate.

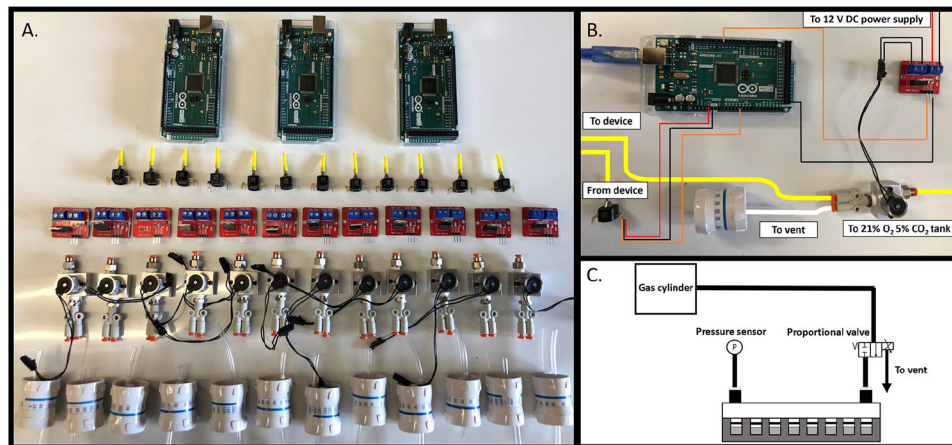


Fig. 2. Device components and wiring. A. Components needed for pressure control device. From top to bottom: Arduino Mega 2560 microcontroller (Qty. 3), piezoresistive pressure sensors (Qty. 12), IRF 520 MOSFET driver modules (Qty. 12), proportional solenoid valves (Qty. 12), and IV flow regulators (Qty. 12). B. Photograph of wiring and pneumatic connections for control of one of twelve pressure conditions. C. Schematic depicting pressure control in one of twelve columns of a 96-well plate.

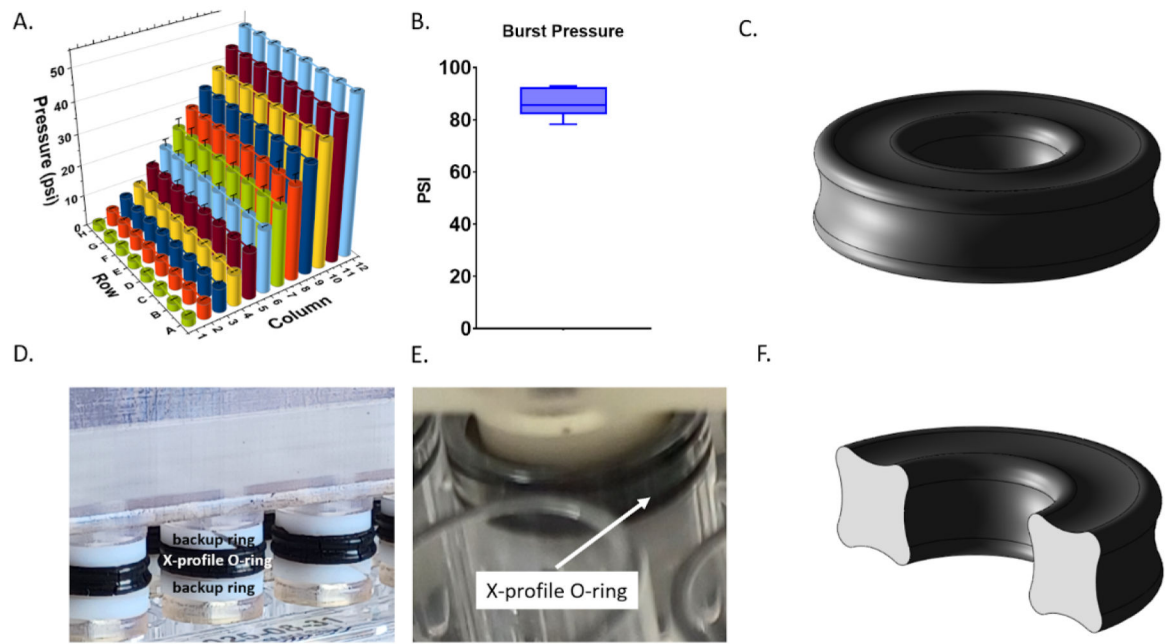


Fig. 3. Device validation and pressure limits. A. Pressure within each well of a 96-well plate. Each column was set to a static pressure ranging from 2.5 to 50 psi. B. Burst pressure of 3D-printed insert device. C. 3D CAD model of X-profile O-ring. D. Photograph of 3D-printed insert device showing PTFE backup rings above and below X-profile O-rings. E. Photograph of device within well of 96-well plate. F. 3D CAD model of cross-section of X-profile O-ring.

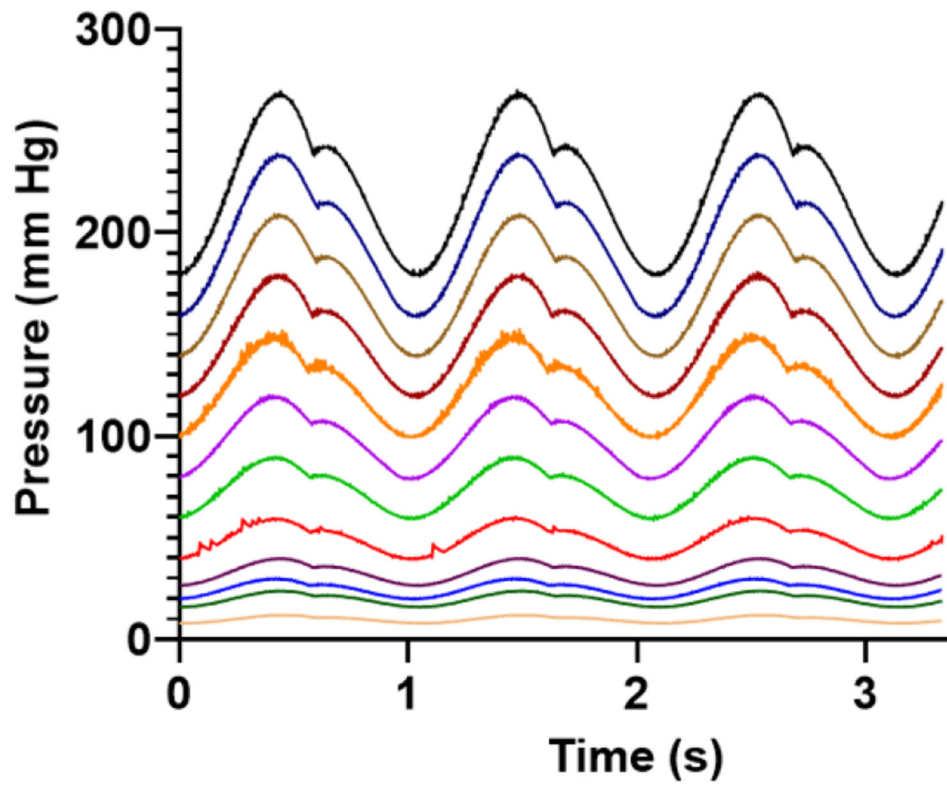


Fig. 4. Twelve physiologic pressure waveforms within a single 96-well plate. Each waveform was generated by multiplying a “normotensive” arterial pressure 120/80 waveform by a scaling factor. Pressures ranged from 12/8 mm Hg to 270/180 mm Hg.

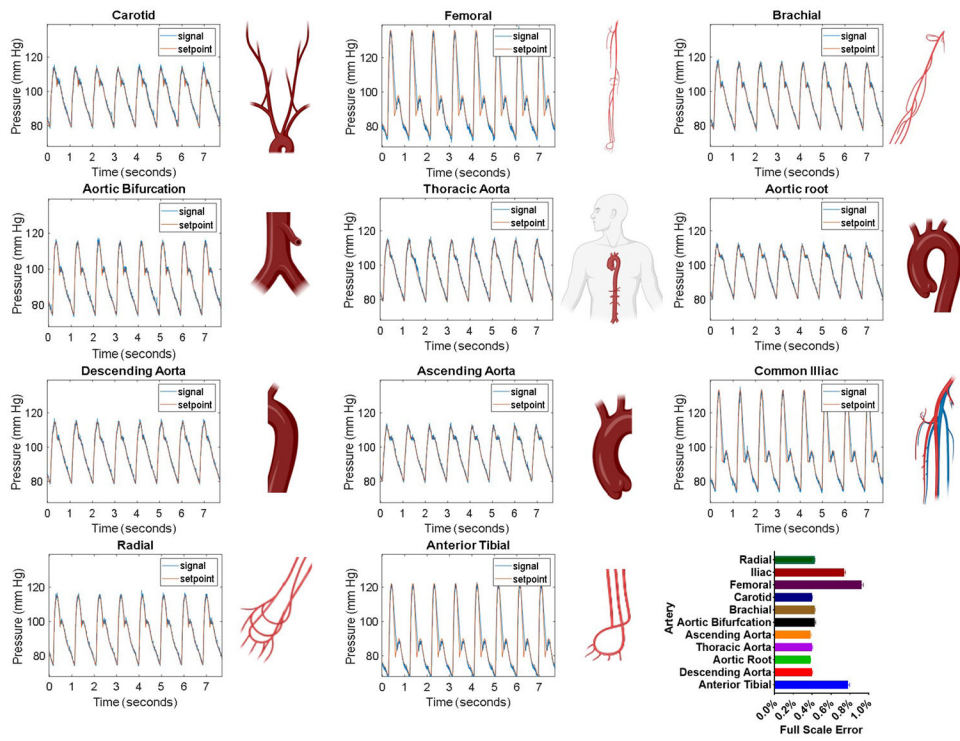


Fig. 5. Patient Waveforms. Patient-derived waveforms. The setpoint values for arterial waveforms 1-11 were taken from a virtual database of normal healthy subjects¹⁴. Generated waveforms (signal, blue line) closely match the setpoint (red line) values and are within 1% full-scale error.

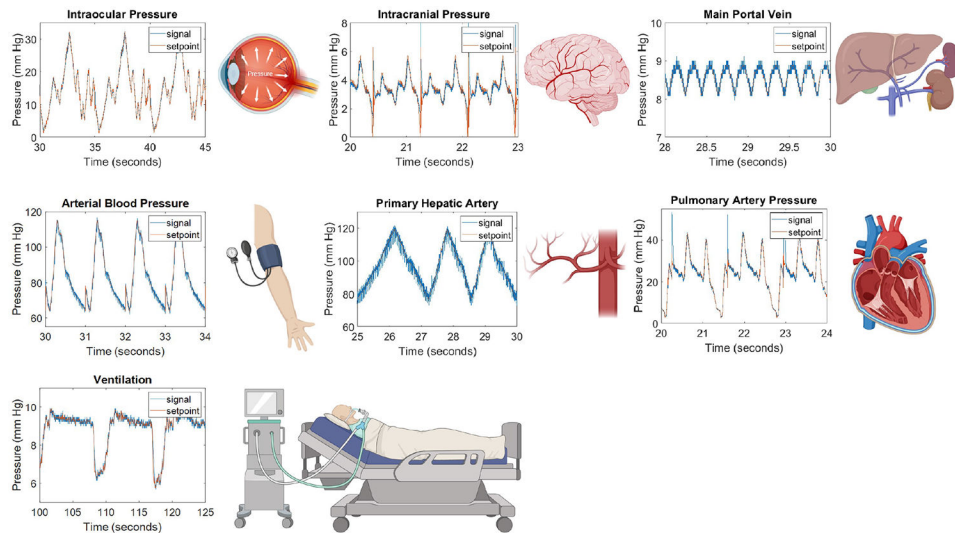


Fig. 6. Patient waveforms derived from clinical databases and journal articles. Waveforms produced by our platform, signal (blue line), closely match setpoint values (red line). Abbreviations: arterial blood pressure (ABP), intracranial pressure (ICP), intraocular pressure (IOP), and pulmonary artery pressure (PAP). Illustrations show from where in the body the pressure waveform occurs.

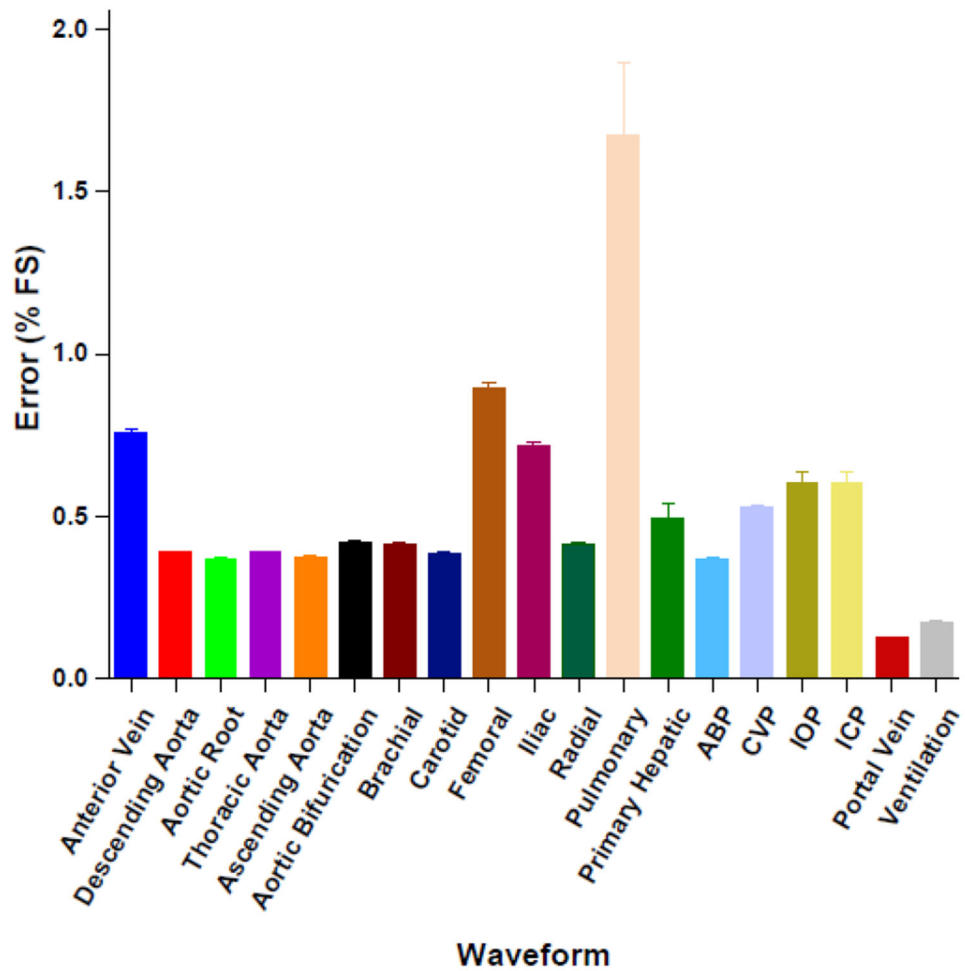


Fig. 7.

Waveform full-scale error. Emulated waveforms are all within 1% full-scale error of setpoint values except pulmonary artery pressure (PAP), which has full-scale error of 1.67%. Abbreviations: arterial blood pressure (ABP), intracranial pressure (ICP), intraocular pressure (IOP), and pulmonary artery pressure (PAP).

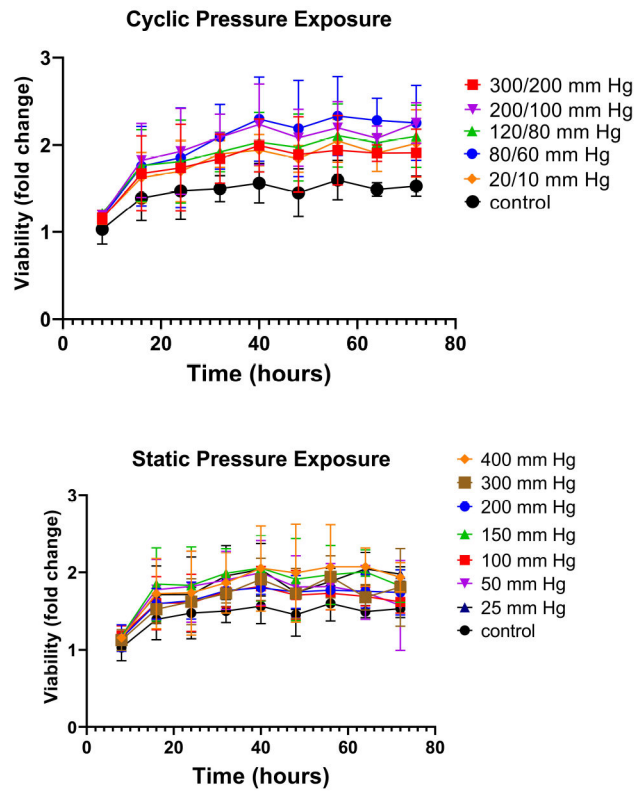


Fig. 8. Cell viability under pressure. HUVECs in each column of a multiwell plate were grown under a unique pressure condition for 3 days. A. Cyclic pressure conditions at 1 Hz. B. Static pressure conditions.

Table 1

Clinical waveforms obtained from databases and journal articles

Waveform	Source/Database	Raw Data/ Digitized	Notes	Reference
Pulmonary artery pressure (PAP)	MGH/MF Database	Raw Data	47 y/o female. Record # mgh 003	16
Central venous pressure (CVP)	MGH/MF Database	Raw Data	47 y/o female. Record # mgh 003	16
Arterial blood pressure	MIMIC-III Database	Raw Data	Arterial line	16-18
Intracranial pressure (ICP)	CHARIS Database	Raw Data	Intraparenchymal	15,16
Intraocular (IOP)	Medical journal	Digitized	Dynamic Intraocular Pressure Measurements During Vitrectomy	19
Common hepatic artery	Academic journal	Digitized	Simulated based on physiological data.	20
Portal Vein	Academic journal	Digitized	Simulated based on physiological data.	20
Ventilator	CPAP Pressure and Flow Data from a Local Trial of 30 Adults at the University of Canterbury.	Raw Data	PEEP 7 cm H ₂ O long breaths	16,21
Anatomy-specific arterial pressure waveforms	Database of virtual healthy subjects.	Raw Data	Simulated based on physiological data	14